Environmental Science & Technology

pubs.acs.org/est

Article

Seasonal Divergence between Microbiomes on Microplastics and Natural Particles Increases with Rising Water Temperatures in Urban Rivers

Yingyu Bao, Yuen-Wa Ho, Zhiyong Shen, Edmund Y. Lam, James K. H. Fang,* Kenneth M. Y. Leung, and Patrick K. H. Lee*

Cite This: *Environ. Sci. Technol.* 2026, 60, 14712−14725

Read Online

ACCESS | Metrics & More | Article Recommendations | Supporting Information

ABSTRACT: The "plastisphere," which comprises microplastics (MPs)-associated microbial communities, is an emerging component of urban river ecosystems. However, its seasonal dynamics remain poorly understood, especially compared with microbiomes on natural particles (NPs). We therefore conducted a year-long metagenomic study at 15 sites across 10 major urban rivers in Hong Kong to compare MP- and NP-associated microbiomes across four seasons. Representative high-quality metagenome-assembled genomes revealed significant seasonal variations in both taxonomic and functional compositions across particle types, with water temperature identified as the primary environmental driver. As temperatures increased, both MP and NP microbiomes exhibited increased taxonomic and functional diversity but reduced functional redundancy and network stability. Compared to NPs, MP microbiomes exhibited higher taxonomic and functional turnover, more complex and connected cooccurrence networks, and distinct taxonomic and functional traits along the temperature gradient. In MP microbiomes, warmer conditions were associated with a higher abundance of pollutant-degrading and putatively virulent taxa (particularly from Firmicutes and Actinobacteria), along with enhanced biosynthetic functions and increased potential microbial sharing and horizontal gene transfer with surrounding aquatic microbiomes. These findings highlight the temperature-dependent ecological impacts of MP microbiomes and underscore the need to consider climatic factors when assessing the long-term ecological risks of MPs in urban riverine ecosystems.

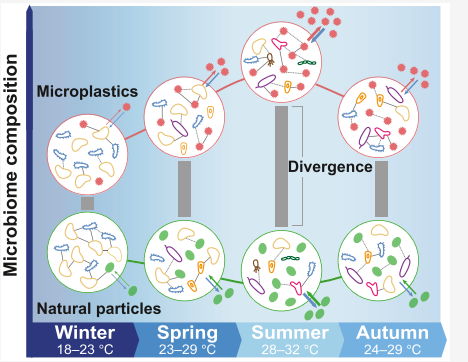

KEYWORDS: *urban rivers, microplastics, plastisphere, seasonal dynamics, water temperature, microbial sharing*

INTRODUCTION

Urban rivers provide crucial ecological services[1] but are threatened by anthropogenic pollution.[2] Microbial communities essential for ecosystem functioning and biodiversity are especially sensitive.[3] Microplastics (MPs), defined as synthetic plastic particles <5 mm, in urban rivers are a major emerging concern.[4,5] MP accumulation introduces novel surfaces for microbial colonization and biofilm formation, collectively known as the "plastisphere[6]". MPs have physicochemical properties distinct from those of natural particles (NPs)[7] and host microbiomes with unique taxonomic and functional traits,[8] which can influence the ecological fates of MPs and broaden their environmental impacts in riverine ecosystems.[9]

Alongside anthropogenic disturbances, urban rivers are shaped by natural seasonal cycles that alter environmental conditions, including water temperature, flow regimes, and nutrient availability.[10,11] These shifts affect microbial activity, community composition, and interactions, with important implications for microbiome dynamics[12] and ecosystem health.[13−15] Although the seasonal dynamics of microbiomes on MPs[16] and NPs[17] have been studied independently, direct comparisons are lacking. Given their distinct physicochemical properties, MPs may exhibit differing seasonal microbiome variability compared to NPs—an important distinction for identifying MP-specific ecological impacts amid broader environmental changes. Moreover, the plastisphere remains connected to the surrounding river water (RW) through continuous microbial sharing at the water−particle interface,[18] which may facilitate the sharing of plastisphere-specific taxonomic and functional traits with the broader riverine microbiome, potentially amplifying MP-specific impacts. However, the mechanisms and extent of such trait sharing under seasonal dynamics remain poorly understood, highlighting the need to investigate plastisphere−environment interactions across seasons.

Received: October 2, 2025
Revised: April 29, 2026
Accepted: April 30, 2026
Published: May 12, 2026

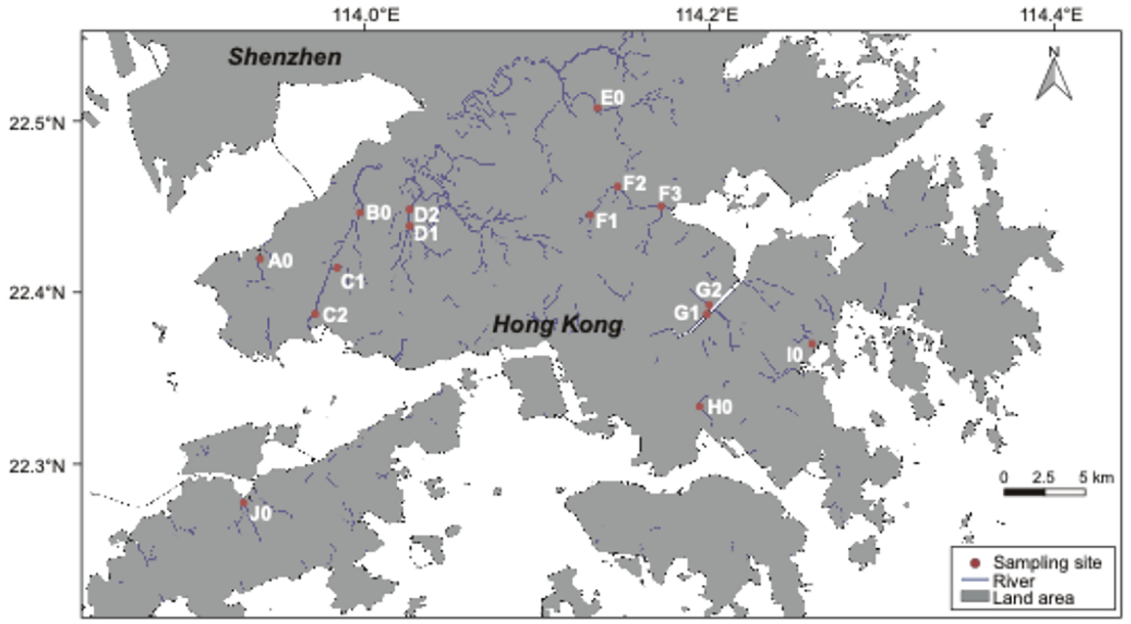

Figure 1. Map of the 15 sampling sites across 10 urban rivers in Hong Kong. Multiple sites within the same river are labeled numerically from upstream to downstream. Reproduced from ref8. Copyright 2025 American Chemical Society.

We hypothesize that seasonal shifts shape microbial assemblages on both MPs and NPs; however, the distinct physicochemical properties of MPs modulate the plastisphere's responses, resulting in season-dependent trait profiles and potential downstream effects on RW through microbial trait sharing. We conducted a year-round metagenomic study of 10 major urban rivers in Hong Kong with pronounced seasonal environmental variations. We reconstructed high-quality representative metagenome-assembled genomes (rMAGs) from MPs, NPs (100−5000 μm), and RW collected at the same locations across the seasons to represent their associated microbial communities, hereafter referred to as microbiomes. We compared seasonal variations in rMAG composition, functional potential, and interrelationships between MPs and NPs; identified season-specific taxonomic and functional traits; and examined the extent and mechanisms of potential trait sharing between particle-associated microbiomes and RW. This study reveals how seasonal dynamics shape MP-associated microbiomes and underscores the importance of climatic variability when assessing MP pollution in riverine ecosystems.

MATERIALS AND METHODS

Two 50-L surface water samples (depth: 0−20 cm) were collected from 15 sites across 10 major urban rivers in Hong Kong at approximately 3-month intervals throughout 2023, corresponding to the four meteorological seasons (Figure 1, Table S1), and were filtered on-site using stainless steel sieves. Retained particles (100−5000 μm) and filtered RW were used for (1) MP, NP, and RW microbiome analysis and (2) MP and NP characterization and quantification. Detailed sample collection, particle characterization, and physicochemical analysis procedures are provided in Text S1. For microbiome analysis, MPs and NPs were nondestructively sorted under a stereomicroscope (SMZ1270i; Nikon, Tokyo, Japan), confirmed via optical photothermal infrared (O-PTIR) spectroscopy (mIRage IR microscope; Photothermal Spectroscopy Corp., Santa Barbara, CA, USA), and then pooled (≥30 particles per sample) to represent MP and NP microbiomes. RW microbiomes were collected on 0.2 μm poly(ether sulfone) filters (Pall Corporation, Port Washington, NY, USA). For characterization, NPs were visually counted and categorized by type and size under a stereomicroscope. For MP characterization, a separate set of particles underwent chemical digestion, after which the remaining particles were analyzed for polymer composition via μ-Raman spectroscopy (inVia confocal Raman microscope; Renishaw, Wotton-under-Edge, UK). MP shapes and sizes were measured under a stereomicroscope, and plastic additives and aging signs were assessed using O-PTIR spectroscopy with a quantum cascade laser microscope.[19,20] Particle surface roughness was examined using a 3D laser microscope (VK-X200, KEYENCE Corporation, Itasca, IL, USA). Concentrations are reported as the number of particles per liter. Field controls showed no evidence of airborne contamination, while laboratory controls indicated minimal background contamination (100−5000 μm; 0.015 ± 0.05 particles/L) and high recovery rates from spike-in experiments for 50-μm (95.0 ± 2.5%) and 500-μm MPs (96.7 ± 2.7%).

The site and seasonal environmental conditions were characterized by using total MP concentrations and 11 physicochemical factors: water temperature, velocity, average daily precipitation, dissolved oxygen, salinity, pH, turbidity, chemical oxygen demand (COD), total phosphorus (TP), total nitrogen, and sulfate. Analytical methods and results are provided in Table S1.

Genomic DNA was extracted from 180 samples (60 each for MP, NP, and RW microbiomes, collected at 15 sites across four seasons) and sequenced. The raw sequences were deposited in the NCBI Sequence Read Archive (BioProject Accession Numbers PRJNA1159715 and PRJNA1330252) and processed for downstream bioinformatic analysis (see Text S2). Key scripts for bioinformatic processing are publicly available at https://github.com/yingyu-best/microplastic-and-natural-particle-microbiome. High-quality reads were obtained through quality control, followed by contig assembly and metagenome-assembled genome (MAG) reconstruction. High-quality MAGs (≥90% completeness, ≤5% contamination) from all samples were dereplicated at a 99% average nucleotide identity (ANI) threshold to generate rMAGs, which were taxonomically and functionally annotated. Unless otherwise stated, all downstream analyses were based on rMAG-resolved microbiomes.

To investigate microbial interrelationships, rMAG cooccurrence networks of MP and NP microbiomes were constructed for each season (see Text S3). Taxonomic traits were identified through indicator analysis; functional traits were characterized using functional indicators to infer life-history strategies (Y−A−S framework)[21] and ecological roles related to biochemical cycling, plastic degradation,

https://doi.org/10.1021/acs.est.5c13903
Environ. Sci. Technol. 2026, 60, 14712−14725

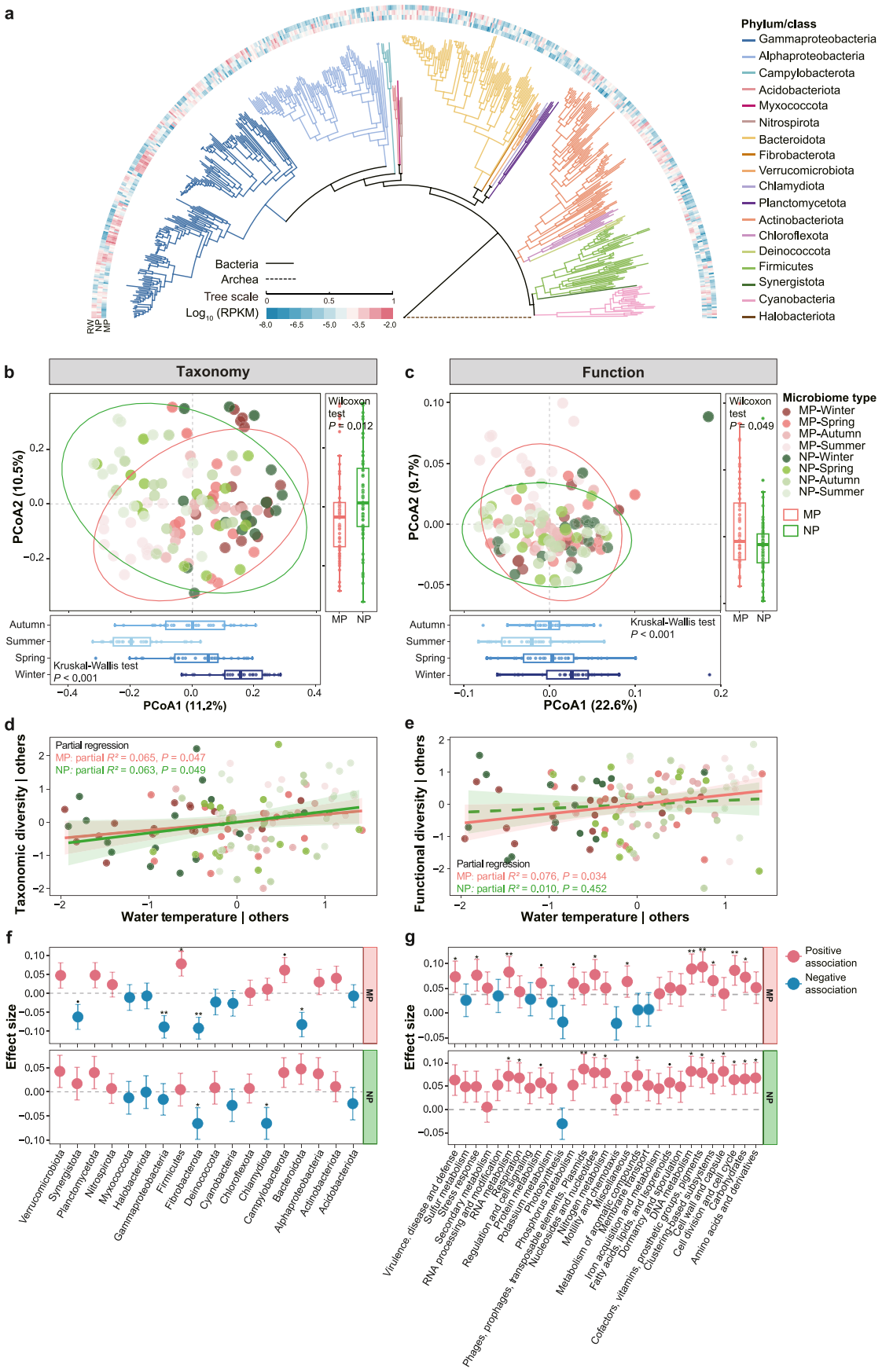

Figure 2. Seasonal variation in the taxonomic and functional compositions of MP and NP microbiomes. (a) Phylogenic tree of high-quality representative metagenome-assembled genomes (rMAGs) at the phylum level (class level for Proteobacteria). Branch colors indicate phylum/class; the heatmap shows the average relative abundance of each rMAG in MP, NP, and RW microbiomes across seasons. (b, c) Principal coordinate

https://doi.org/10.1021/acs.est.5c13903
Environ. Sci. Technol. 2026, 60, 14712−14725

Figure 2. continued

analysis (PCoA) of (b) taxonomic and (c) functional composition based on Bray−Curtis dissimilarity. Boxplots show sample distributions along PCoA1 and PCoA2 by season and microbiome type, respectively. Two distinct color schemes are used to differentiate microbiome types, while the color intensity (from dark to light) indicates seasonal progression, corresponding to increasing temperatures. Ellipses represent 95% confidence intervals. (d, e) Partial regression analyses showing relationships between water temperature and the (d) taxonomic and (e) functional diversity indices in MP and NP microbiomes after controlling for confounding variables. Shaded areas indicate 95% confidence intervals from linear regression models. (f, g) Effects of water temperature on the relative abundance of (f) each phylum (class for Proteobacteria) and (g) functional categories in MP and NP microbiomes, based on linear mixed models. Color indicates the direction of association with water temperature (positive or negative) (***$P < 0.001$; **$P < 0.01$; *$P < 0.05$; ·$P < 0.1$).

and antibiotic resistance and putative virulence (see Text S4). rMAGs with a population-level ANI ≥99.999% between MPs or NPs and RW at the same site or river were interpreted as evidence of microbial sharing;[22,23] potential horizontal gene transfer (HGT) events were predicted among taxonomic indicators and other shared rMAGs (see Text S5). The effects of water temperature, particle type, and microbiome attributes (diversity, stability, trait abundance) on trait sharing between particles and RW were evaluated via partial least-squares path model (PLS-PM) analysis (see Text S6).

All data analyses and statistical tests were performed in *R* (v.4.1.1)[24] (see Text S7). Taxonomic and functional compositions were visualized using principal coordinate analysis (PCoA), and compositional differences between two microbiome types or seasons were assessed using pairwise permutational multivariate analysis of variance (PERMANOVA) and permutational analysis of multivariate dispersion (PERMDISP). Associations between rMAG and short-read taxonomic compositions were evaluated via Procrustes analysis.[25] Associations between environmental factors and microbial composition were evaluated via distance-based redundancy analysis (db-RDA) and multiple regressions (MR). Relationships between pairwise similarities in MP characteristics and taxonomic compositions were assessed using Mantel tests. Partial regressions (PR) were used to quantify the individual effects of environmental factors on taxonomic diversity, functional diversity, and redundancy while controlling for confounding variables. Linear regressions (LR) tested relationships between pairwise microbial similarity and temperature differences and between water temperature and network topology in particle microbiomes. Linear mixed-effects models (LMMs), with a sampling site as a random intercept, evaluated the effects of water temperature and particle type on microbiome attributes and shared rMAG numbers. Generalized linear models (GLMs) assessed differences in the presence of functional genes across specific rMAG groups, including taxonomic indicators and shared rMAGs between particle microbiomes. Statistical significance was determined using 999 permutations, with false discovery rate correction. Quantitative results are reported as means ± standard deviations.

RESULTS

Seasonal Variations in Environmental Conditions and Particle Characteristics in Urban Rivers

MP, NP, and RW samples were collected from urban rivers in Hong Kong during four seasons (February, May, August, and October). The average water temperature was lowest in winter (20.2 ± 1.3 °C), increased through spring (26.3 ± 2.1 °C) to a summer peak (29.9 ± 1.0 °C), then decreased in autumn (26.6 ± 1.7 °C) (Figure S1, Table S1). Daily average precipitation was significantly higher in spring and summer than in winter and autumn (Wilcoxon test, all $P < 0.01$). Other environmental factors remained relatively stable across seasons, except for COD, which was significantly higher in winter than in summer and autumn (Wilcoxon test, all $P < 0.05$).

Across seasons, four MP polymer types—polypropylene (PP), polyethylene (PE), polystyrene (PS), and polyethylene terephthalate (PET)—were consistently detected. Average total MP concentrations ranged from 0.9 ± 0.5 (autumn) to 2.5 ± 1.9 particles/L (winter), with a significant difference only between winter and autumn (Wilcoxon test, $P = 0.025$) (Figure S1, Table S1). MPs predominantly comprised PP, in fragment form, with sizes of 100−200 μm across most sites and seasons (Figure S2a−c). Significant seasonal variation in MP composition (polymer type, shape, size) was detected only between winter and other seasons (pairwise PERMANOVA, all $F > 3.829$, $R^2 > 0.120$, $P < 0.01$) (Table S2a). NP concentrations remained stable across seasons and were approximately 5−20 times higher than MP concentrations (Table S1), consistent with previous studies.[26] NP composition (type, size) showed no significant seasonal variation (pairwise PERMANOVA, all $F < 1.846$, $R^2 < 0.062$, $P > 0.05$) (Table S2a). Plant remnants, mosses, and sand (typical size: 200−1000 μm) were the dominant NP types across sites (Figure S2d,e).

Surface analysis revealed plastic additives, including phthalates, slip agents, antioxidants, and hindered amine light stabilizers, across all four MP polymer types (Figure S3a), with stronger signals in warmer seasons (summer and autumn). Seasonal variation in environmental aging was evident and polymer-specific (Figure S3b). In summer, PET exhibited slightly reduced crystallinity, and PS showed signs of surface oxidation, suggesting accelerated aging under warmer conditions. PE and PP showed slight increases in crystallinity in warmer seasons, indicating potential resistance to oxidative degradation. MPs consistently exhibited significantly greater surface roughness than NPs (Wilcoxon test, all $P < 0.05$). Surface roughness varied significantly with season for both particle types (Kruskal−Wallis test, all $P < 0.01$), with higher values in warmer seasons, especially summer (Figure S4). These results highlight the consistently distinct seasonally variable physicochemical properties of MPs and NPs.

Seasonal Variations in MP and NP Microbiomes

To support genome-resolved analyses, we recovered 577 high-quality taxonomically and functionally representative rMAGs across all seasons and microbiome types (Figure 2a); see detailed genome quality statistics and taxonomic and functional assessments in Text S8 and Table S3. Taxonomic and functional compositions were characterized exclusively from these rMAGs, representing rMAG-resolved microbiomes. In both MP and NP microbiomes, the dominant phyla—Proteobacteria, Actinobacteria, and Bacteroidota—and key metabolism-related functional categories (e.g., proteins, carbohydrates, amino acids, and derivatives) and clustering-based subsystems (statistically inferred gene groups with poorly characterized functions) remained consistent across seasons (Figures S5, S6). However, taxonomic and functional compositions varied significantly across seasons and between particle types. Season had a stronger influence on the microbiome taxonomic and functional structure than the particle type (PERMANOVA, all $F > 3.512$, $R^2 > 0.080$, $P =$

https://doi.org/10.1021/acs.est.5c13903
Environ. Sci. Technol. 2026, 60, 14712−14725

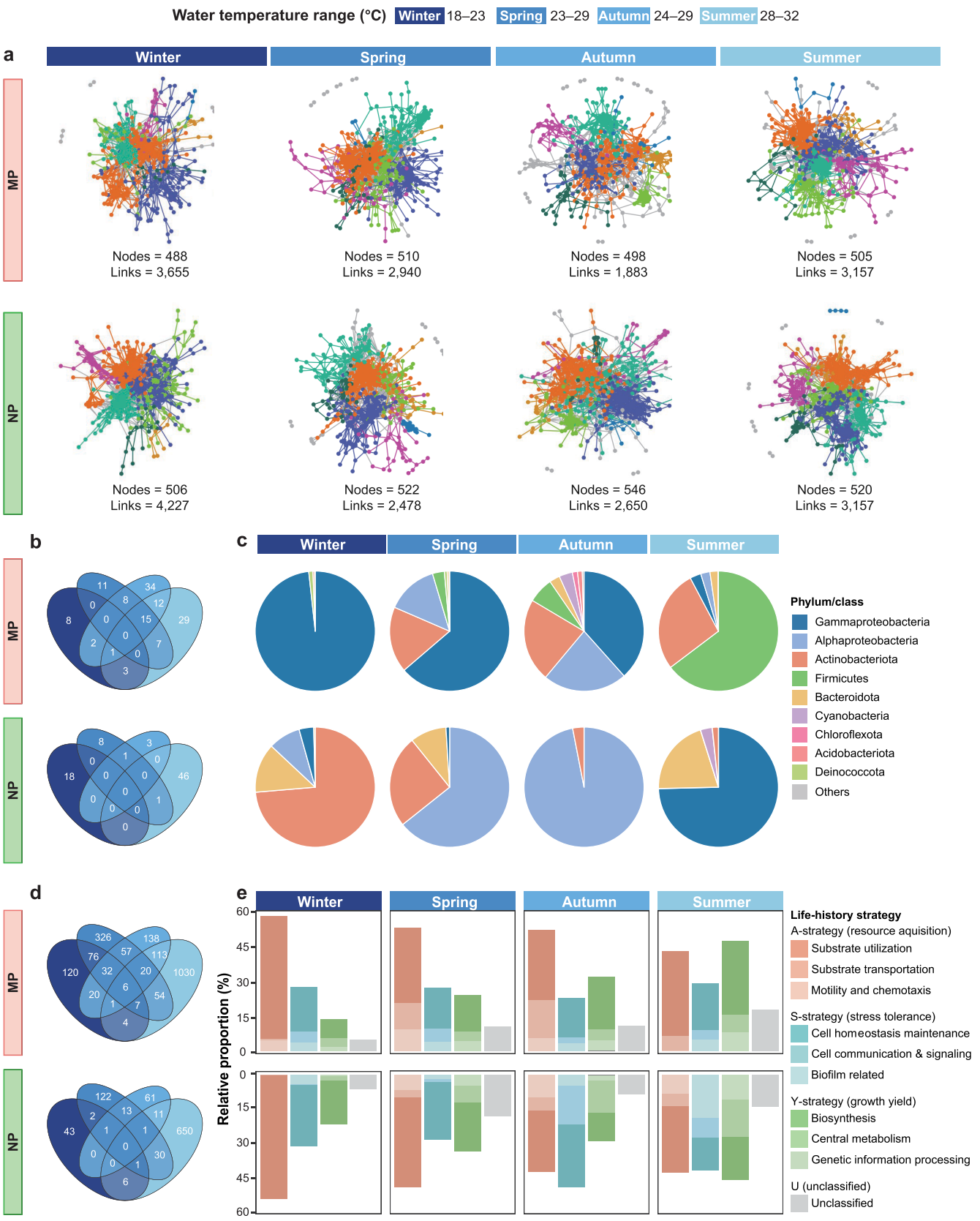

Figure 3. Variations in microbial cooccurrence network topology and taxonomic/functional indicators in MP and NP microbiomes across the water temperature gradient. (a) Seasonal cooccurrence networks of MP and NP microbiomes. The eight largest modules are color-coded; smaller modules are shown in gray. (b, d) Shared and unique (b) taxonomic and (d) functional indicators of MP and NP microbiomes. (c) Average relative proportion of taxonomic indicators at the phylum level (class level for Proteobacteria) based on their relative abundance among all indicator taxa in each microbiome type. Colors indicate different phyla or classes. (e) Average relative proportions of life-history strategies inferred from rMAG-

https://doi.org/10.1021/acs.est.5c13903
Environ. Sci. Technol. 2026, 60, 14712−14725

Figure 3. continued

derived functional indicators, based on their relative abundance among all indicator functions in each microbiome type. Different color schemes denote subcategories within each life-history strategy. Within each panel, seasons are indicated by the color scheme shown at the top of the figure.

0.001), although the latter also had a significant effect (PERMANOVA, all $F < 3.186$, $R^2 < 0.023$, $P < 0.01$) (Table S2b). This pattern was reflected in PCoA: sample separation along the first axes (explaining the most variance) differed significantly by season (Kruskal−Wallis test, all $P < 0.001$), while the second axes captured particle-type differences (Wilcoxon test, all $P < 0.05$) (Figure 2b,c). Significant interactive effects between season and particle type (PERMANOVA, all $F > 1.493$, $R^2 > 0.034$, $P < 0.010$) further indicate seasonal variance in the magnitude and nature of microbiome differences between MPs and NPs. Taxonomic and functional diversity and functional redundancy differed significantly across seasons (Kruskal−Wallis test, all $P < 0.01$) but were comparable between particle microbiomes (Wilcoxon test, all $P > 0.05$), reinforcing the dominance of seasonal variation. In contrast, RW microbiomes exhibited seasonal stability (pairwise PERMANOVA, all $F < 2.363$, $R^2 < 0.078$, $P > 0.05$; pairwise PERMDISP, all $P > 0.05$) and compositions distinct from particle-attached microbiomes (pairwise PERMANOVA, all $F > 2.352$, $R^2 > 0.085$, $P < 0.05$; pairwise PERMDISP, all $P > 0.05$) (Table S2b). Hence, subsequent analyses focused on seasonally variable particle microbiomes.

Water Temperature Drove Distinct Seasonal Variations in MP and NP Microbiomes

To identify environmental drivers of seasonal microbiome variation, 11 measured factors were analyzed using multiple statistical approaches. db-RDA identified water temperature as the strongest predictor of seasonal variations in both particle microbiomes, explaining the largest proportion of taxonomic (multiple regression, all $R^2 > 0.569$, $P < 0.001$) and functional variation (all $R^2 > 0.251$, $P < 0.001$) (Table S4), with sample distributions aligning along the water temperature gradient (Figure S7). Other environmental factors made lesser contributions: in both particle microbiome types, taxonomic variation was associated with precipitation, COD, and TP (all $R^2 < 0.275$, $P < 0.05$), while functional variation was influenced by precipitation and turbidity in MPs (all $R^2 < 0.241$, $P < 0.05$), and by sulfate in NPs ($R^2 = 0.140$, $P = 0.012$) (Table S4). In MP microbiomes, taxonomic and functional compositions varied significantly with total MP concentration (multiple regression, all $R^2 > 0.105$, $P < 0.05$) (Table S4), but not with the relative MP type, shape, or size composition (Mantel test, r: −0.149 to 0.086, all $P > 0.05$) (Table S5).

α-Diversity was also strongly influenced by water temperature, the only factor significantly and positively correlated with taxonomic diversity in both particle microbiomes after controlling for other variables (partial regression, all partial $R^2 > 0.059$, $P < 0.05$) (Figures 2d, S8) and the primary driver of functional diversity in MPs (partial $R^2 = 0.076$, $P = 0.034$) (Figures 2e, S9). Functional redundancy declined significantly with increasing water temperature in both particle microbiomes (all partial $R^2 > 0.068$, $P < 0.05$) (Figure S10). Water velocity also influenced functional diversity and redundancy in MPs, although its effects were minor (all partial $R^2 < 0.076$, $P < 0.05$) (Figures S9, S10). These results identify water temperature as the independent primary environmental driver of seasonal variations in diversity, taxonomic composition, and functional potential in both particle microbiomes. Subsequent analyses focused on microbial responses to water temperature.

Although both particle microbiomes varied with water temperature, MP microbiomes exhibited steeper taxonomic and functional turnover (LR, R^2: 0.033−0.075, slope: −0.009 to −0.003, $P < 0.001$) across a 13.9 °C temperature range, indicating greater compositional shifts along the water temperature gradient (Figure S11). NP microbiomes exhibited milder changes, with lower taxonomic and functional turnover (R^2: 0.013−0.024, slope: −0.005 to −0.002, $P < 0.001$). Water temperature effects also varied across microbial taxa and functional categories. In MP microbiomes, the relative abundances of Gammaproteobacteria and Bacteroidota declined significantly with increasing water temperature (LMM, all $\beta < -0.082$, $P < 0.05$) while that of Firmicutes increased (LMM, $\beta = 0.077$, $P = 0.018$) (Figure 2f). These temperature-associated trends were absent in NP microbiomes: only Chlamydiota declined significantly with increasing water temperature (LMM, $\beta = -0.065$, $P = 0.046$) (Figure 2f). Functionally, stress responses increased with water temperatures only in MP microbiomes (LMM, $\beta = 0.077$, $P = 0.018$) (Figure 2g); metabolism-related categories (e.g., nitrogen, aromatic compounds, and amino acids and derivatives) increased only in NP microbiomes (LMM, all $\beta > 0.068$, $P < 0.05$) (Figure 2g). These results highlight the distinct taxonomic and functional responses of MP and NP microbiomes along the water temperature gradient.

Water Temperature Distinctly Influenced MP and NP Microbiome Network Structure and Stability

Water temperature-driven compositional variations in particle microbiomes may influence their interrelationships and stability. We constructed cooccurrence networks for each microbiome type across seasonal water temperature ranges (Figure 3a). All networks exhibited scale-free, small-world properties, with power-law exponents of 0.685−0.812 and higher modularity and connectivity than those in random networks (Z-test, all $P < 0.05$) (Table S6).

Particle microbiomes exhibited distinct cooccurrence responses to water temperature (LMM, β: −0.978 to 0.892, $P < 0.001$) (Figure S12a). In MP microbiomes, subnetwork connectivity and complexity increased with water temperature, indicated by more nodes and links, higher connectance and average node degrees, and shorter diameter and average path lengths (LR, all $R^2 > 0.063$, $P < 0.05$) (Figure S13a). NP subnetworks exhibited the opposite trends (except for total node number) (Figure S13a), indicating reduced complexity at higher water temperatures.

In both microbiomes, subnetwork stability declined with increasing water temperature, reflected by reduced robustness (random and targeted; LMM, all $\beta < -0.284$, $P < 0.001$) and increased vulnerability (LMM, $\beta = 0.319$, $P = 0.004$) (Figures S12b, S13b). The absolute ratio of negative-to-positive cohesion, which proxies for competitive versus cooperative interactions, declined with increasing water temperature in both particle microbiomes (LMM, $\beta = -0.271$, $P < 0.001$), supporting reduced stability. Although these trends did not differ significantly between particle types (LMM, β: −0.252 to

https://doi.org/10.1021/acs.est.5c13903
Environ. Sci. Technol. 2026, 60, 14712−14725

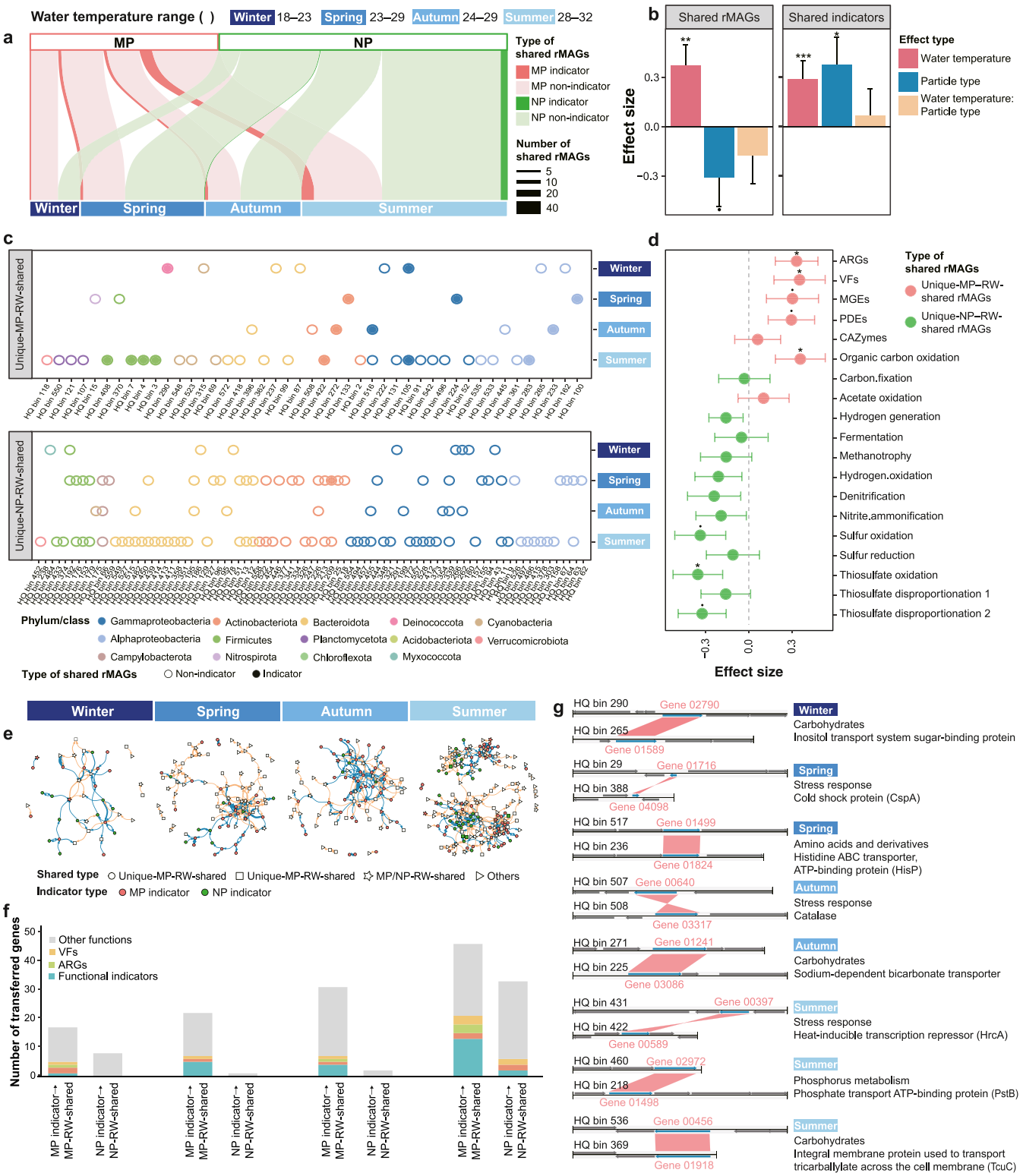

Figure 4. Microbial sharing and horizontal gene transfer (HGT) in MP and NP microbiomes across the water temperature gradient. (a) Shared rMAGs between MPs or NPs and RW across the water temperature gradient. The width of each band connecting two environments represents the number of shared rMAGs; the color indicates whether they are taxonomic indicators. (b) Independent and interactive effects of water temperature and particle type on the numbers of shared rMAGs and shared taxonomic indicators, based on linear mixed models. (c) Seasonal taxonomic compositions of rMAGs uniquely shared between MPs and RW (unique-MP−RW-shared) and NPs and RW (unique-NP−RW-shared). Filled and unfilled symbols represent taxonomic indicators and non-indicators, respectively, with colors indicating phylum (class level for Proteobacteria). (d) Differences in ecological roles between unique-MP−RW-shared and unique-NP−RW-shared rMAGs based on generalized linear models. Dots to the left or right of the vertical dashed line denote functions enriched in unique-NP−RW-shared or unique-MP−RW-shared rMAGs, respectively (*** $P < 0.001$; ** $P < 0.01$; * $P < 0.05$). (e) HGT networks among shared rMAGs and taxonomic indicators, identified within each season. The node shape denotes the shared rMAG type; fill color denotes the indicator type. Arrows indicate the gene transfer direction. (f) Counts of genes

https://doi.org/10.1021/acs.est.5c13903
Environ. Sci. Technol. 2026, 60, 14712−14725

Figure 4. continued

horizontally transferred from taxonomic indicators to other shared rMAGs, identified within each season. Arrows indicate the gene transfer direction, and colors represent functional groups. (g) Representative examples (n = 4) of MP functional indicators identified in summer that were transferred via HGT from taxonomic indicators to other shared rMAGs; full details are provided in Table S10. ARGs: antibiotic resistance genes; VFs: virulence factors; MGEs: mobile genetic elements; PDEs: putative plastic degradation enzymes; CAZymes: carbohydrate-active enzymes.

0.258, $P > 0.05$), absolute negative cohesion decreased significantly only in MP microbiomes (LR, R^2 = 0.050, P = 0.047), suggesting that MP microbial networks may be more vulnerable to water temperature-driven destabilization than NP networks.

Varying Taxonomic and Functional Traits of MP Microbiomes along the Water Temperature Gradient

To identify traits along the water temperature gradient, taxonomic and functional indicators distinguishing particle microbiomes within each season were identified based on differences in relative abundance and occurrence frequency (Figure 3b,d, Tables S7, S8). In both microbiome types, few indicators overlapped across seasons, reflecting a strong seasonal variation. The numbers of taxonomic and functional indicators increased with water temperature, peaking in summer, decreasing in autumn and spring, and reaching the lowest levels in winter. MP microbiomes consistently exhibited more taxonomic and functional indicators than NP microbiomes across most seasons, indicating greater divergence with a rising water temperature in the former.

The taxonomic indicator composition in both particle microbiomes shifted with the water temperature gradient (Figure 3c, Table S7). In MP microbiomes, warmer conditions drove a transition from Gammaproteobacteria to Firmicutes and Actinobacteria (Figure 3c), with enrichment of fecal indicators and putative pathogens (e.g., *Enterococcus*, *Escherichia*, and *Staphylococcus*)[27] and pollutant-tolerant or degrading taxa (e.g., *Gordonia*,[28] *Nocardioides*,[28] and *Corynebacterium*[29]) commonly associated with wastewater treatment systems (Figure S14). Despite seasonal variations, MP taxonomic indicators consistently included potential plastic degraders, with dominant genera (e.g., *Massilia*,[30] *Pseudomonas*,[31] *Acinetobacter*,[32] and *Exiguobacterium*[33]) shifting between seasons (Figure S14). NP taxonomic indicators shifted from Actinobacteria to Alphaproteobacteria and then Gammaproteobacteria with increasing water temperature (Figure 3c). Although dominant NP indicator genera varied seasonally (e.g., *Microbacterium*,[34] *Sphingomonas*,[35] and *Sphaerotilus*[36]), all were functionally linked to carbohydrate utilization (Figure S14).

Functional indicators also reflected water temperature-driven shifts in life-history strategies (Figure 3e, Table S8). With warming, both particle microbiomes transitioned from A-strategies (resource acquisition) to Y-strategies (growth yield), indicating enhanced growth potential (Figure 3e). At higher water temperatures, MP microbiomes invested more in biosynthesis (e.g., amino acids, proteins, cofactors), whereas NP microbiomes favored central metabolic respiration. These distinct Y-strategy functions highlight divergent resource allocation: MP and NP prioritize cellular synthesis and energy production, respectively (Figures 3e, S15). A-strategy functions (e.g., carbohydrate and amino acid utilization, iron acquisition) remained more prevalent in MP microbiomes across all water temperatures (Figure 3e), but their relative proportions among all functional indicators declined with warming (Figure S15). S-strategy functions (stress tolerance) were dominated by cell homeostasis in both microbiomes, with MP microbiomes showing greater enrichment in DNA repair and resistance to antibiotics and other bioactive compounds (Figures 3e, S15). In summer, the biofilm-related functions quorum sensing and regulation and EPS biosynthesis and modification contributed differently to S-strategy functions in MP and NP microbiomes, and both increased with water temperature (LR, all $R^2 > 0.035$, $P < 0.1$) (Figure S16). Notably, 27.1−58.6% of functional indicators in MP and 17.0−50.0% in NP microbiomes were significantly more frequently carried by their corresponding taxonomic indicators (GLM, all $|\beta| > 0.222$, $P < 0.05$), highlighting how taxonomic shifts drive functional divergence (Figure S17).

Beyond indicator-based functional traits, several microbiome functions crucial for riverine ecosystem function and health were significantly shaped by water temperature and/or particle type (Figure S18). Functions related to putative virulence, complex carbohydrate degradation, denitrification, organic carbon oxidation, and fermentation increased significantly with water temperature in both particle microbiomes (LMM, all $\beta > 0.189$, $P < 0.01$), with the first three slightly more abundant in MP microbiomes (LMM, all $\beta > 0.264$, $P < 0.1$). Those related to antibiotic resistance and plastic degradation were consistently more abundant in MP microbiomes (LMM, all $\beta > 0.378$, $P < 0.05$) but unaffected by water temperature (LMM, all $\beta < 0.207$, $P > 0.1$), suggesting persistent functional specialization in MP microbiomes across the water temperature gradient.

Water Temperature Influenced Potential Trait Sharing between MP and RW Microbiomes

Given the distinct water temperature-driven shifts in particle microbiomes, we compared their potential to share microbes with RW microbiomes along the water temperature gradient. We identified 122 and 160 potentially shared rMAGs between MPs and RW (i.e., MP−RW-shared) and between NPs and RW (i.e., NP−RW-shared), respectively, based on cooccurrence within the same sampling site or river (Table S9); these corresponded to 240 MP−RW and 365 NP−RW sharing events across all sites and rivers along the water temperature gradient (Figure 4a). The number of shared rMAGs per site or river increased significantly with water temperature for both microbiome types (LMM, β = 0.376, $P < 0.001$) (Figure 4b).

Despite comparable numbers of MP−RW-shared and NP−RW-shared rMAGs per site (LMM, β = −0.309, P = 0.080) (Figure 4b), their taxonomic and functional compositions differed markedly. Over half of the shared rMAGs were either unique-MP−RW-shared (n = 45) or unique-NP−RW-shared (n = 83); only 77 rMAGs were shared by both microbiomes (i.e., MP/NP−RW-shared). Unique-MP−RW-shared rMAGs included members found exclusively in Deinococcota, Nitrospirota, and Planctomycetota (Figure 4c). Functionally, unique-MP−RW-shared rMAGs carried significantly more antibiotic resistance genes (ARGs), virulence factors (VFs), and organic carbon oxidation-related genes than their NP

https://doi.org/10.1021/acs.est.5c13903
Environ. Sci. Technol. 2026, 60, 14712−14725

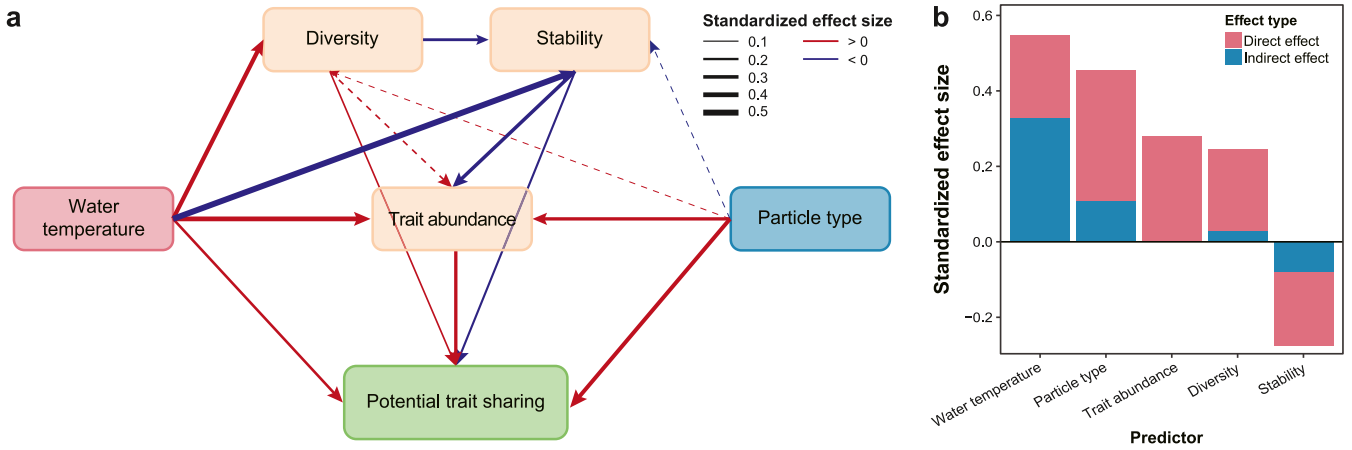

Figure 5. Potential mechanisms underlying trait sharing between MP- or NP-associated and RW microbiomes. (a) Partial least-squares path model (PLS-PM) illustrating the relationships among water temperature, particle type, microbial assemblage attributes, and trait sharing with RW. Solid and dashed arrows indicate significant and nonsignificant paths, respectively. Arrow colors denote positive or negative effects, and line thickness reflects the standardized effect size. (b) Standardized total effects (sum of direct and indirect effects) derived from the PLS-PM.

counterparts (GLM, $\beta > 0.334$, $P < 0.05$), along with marginally higher levels of mobile genetic elements and putative plastic-degrading enzymes (PDEs; GLM, $\beta > 0.315$, $P < 0.1$) (Figure 4d).

To investigate potential sharing of temperature-specific microbial traits, we identified taxonomic indicators shared between MPs or NPs and RW within each seasonal water temperature range. Although these accounted for a small fraction of total sharing events (Figure 4a), their contributions increased significantly with water temperature (LMM, $\beta = 0.288$, $P < 0.001$), suggesting enhanced trait-sharing potential under warmer conditions. Importantly, MP microbiomes contributed significantly more unique taxonomic indicators to RW than NP microbiomes (15 MP indicators versus 1 NP indicator; Figure 4b). The number of trait-sharing events also increased with water temperature (Figure 4c). These findings suggest that MPs have a greater capacity to share unique microbial traits with RW microbiomes, particularly at elevated water temperatures.

MPs and NPs also may facilitate the transfer of functional traits to RW microbiomes via HGT between taxonomic indicators and other shared rMAGs within each seasonal water temperature range. The highest number of HGT events was associated with particle taxonomic indicators under high temperatures (summer, $n = 386$), followed by moderate (autumn: $n = 165$; spring: $n = 159$) and low temperatures (winter, $n = 62$) (Figure 4e). Across all seasons, MP taxonomic indicators contributed more HGT events to other MP−RW-shared rMAGs ($n = 17$ to 46) than NP indicators did to other NP−RW-shared rMAGs ($n = 1$−33) (Figure 4f). Transferred MP functional traits included functional indicators primarily linked to metabolism (e.g., carbohydrates, phosphorus, amino acids, and derivatives), stress responses (e.g., heat shock, cold shock, oxidative stress), and putative PDEs, VFs, and ARGs, mainly contributed by MP taxonomic indicators under warmer conditions (Figure 4f,g, Table S10). In contrast, HGT of NP functional traits was limited and occurred exclusively from taxonomic indicators under warm conditions (Figure 4f).

Mechanisms Driving Trait Sharing between MP and RW Microbiomes

To investigate trait-sharing mechanisms between particle-associated and RW microbiomes, including taxonomic indicator sharing and gene transfer from taxonomic indicators to other shared rMAGs, a PLS-PM incorporating water temperature, particle type, and microbiome attributes (i.e., microbial diversity, stability, relative abundance of unique taxonomic and functional traits) was constructed. The PLS-PM yielded good performance (goodness-of-fit = 0.487) and standardized effect sizes (β) comparable to those from a structural equation model accounting for the sampling site as a random effect (Figures 5a, S19c,d), indicating minimal site-specific influence and supporting model robustness.

The PLS-PM results reveal that water temperature was the primary driver of microbiome attributes in both particle communities (Figure 5a, Table S11). As water temperature increased, microbial diversity ($\beta = 0.365$, $P < 0.001$) and trait abundance ($\beta = 0.398$, $P < 0.001$) increased, while microbial stability decreased ($\beta = -0.495$, $P < 0.001$). Particle type significantly influenced only trait abundance, with MPs supporting a higher abundance of unique traits than NPs ($\beta = 0.275$, $P < 0.001$). Microbiome attributes were interrelated: diversity negatively affected stability ($\beta = -0.232$, $P = 0.004$), while stability was negatively associated with trait abundance ($\beta = -0.304$, $P = 0.001$). Overall, the potential for trait sharing, measured using the number of taxonomic indicators involved, was significantly influenced by all assessed factors (β: −0.184 to 0.348, all $P < 0.05$), with water temperature and particle type exerting the strongest total effects (Figure 5b). Water temperature had a stronger indirect ($\beta = 0.341$) than direct effect ($\beta = 0.205$), while the particle type had a stronger direct ($\beta = 0.348$) than indirect effect ($\beta = 0.107$) (Figure 5b), highlighting the greater indirect influence of temperature on microbial community composition.

DISCUSSION

Seasonal environmental variability, modulated by the persistence of MPs and urban river dynamics, shapes the plastisphere.[37] Despite reports of distinct taxonomic and functional traits in the plastisphere (vs NPs),[8] it remains unclear whether these differences are seasonal. Seasonal dynamics are key to distinguishing MP-specific microbial responses from those driven by broader environmental factors. We seasonally analyzed MP- and NP-associated microbiomes in 10 urban rivers in Hong Kong for one year. Seasonal

https://doi.org/10.1021/acs.est.5c13903
Environ. Sci. Technol. 2026, 60, 14712−14725

variation, particularly in water temperature, was the primary driver of taxonomic and functional shifts in both particle types, which responded similarly in terms of diversity, stability, and extent of rMAG sharing with RW microbiomes. Significant interactive effects between water temperature and particle type were observed: compared with NP microbiomes, as water temperatures increased, MP microbiomes exhibited greater taxonomic uniqueness, distinct life-history strategies, and a higher potential for microbial sharing and HGT with RW microbiomes.

The increased taxonomic and functional diversity in both particle-associated microbiomes is likely to be due to the dominance of rising water temperatures in expanding ecological niches,[38] although other factors (e.g., water velocity) may have contributed. These temperature-driven changes were accompanied by a shift from A- to Y-strategic taxa, consistent with reduced nutrient limitation.[21] This pattern may reflect enhanced riverine primary productivity under warmer conditions,[39] which increases nutrient availability and supports the metabolic activity and growth of diverse taxa in both microbiomes.[40,41] In Hong Kong, warmer periods typically coincide with increased rainfall driven by the summer monsoon, which introduces exogenous microbes from tributaries and wastewater runoff,[42] enriching sewage-associated taxonomic indicators (e.g., Firmicutes[43] in MP microbiomes, Bacteroidota[43] in NP microbiomes) and elevating VF abundances. However, higher water temperatures also promote niche partitioning, evidenced by decreasing functional redundancy in both microbiomes, which may weaken the ability to buffer taxon loss and decrease stability and stress resilience.[44] Lower redundancy may also reduce competitive interactions,[45] indicated by decreasing absolute negative-to-positive cohesion ratios.[46] Negative cohesion helps contain environmental disturbances within microbial networks;[47] its decline suggests destabilized interrelationships and reduced robustness under warmer conditions. Such conditions also may have enhanced microbial movement in search of favorable habitats.[18,48] Reduced microbiome stability may have facilitated particle colonization by exogenous RW microbes,[49] causing both particle microbiomes to increase microbial sharing with RW, with potential long-term impacts on riverine microbial composition and function.

Although water temperature influenced both particle-associated microbiomes, the extent and nature of their taxonomic and functional shifts differed, reflecting particle-specific microbial responses. Compared with NP microbiomes, MP microbiomes exhibited greater taxonomic and functional turnover and more indicator taxa and functions across the water temperature gradient. Network analysis revealed distinct patterns of increased connectivity and reduced modularity in MP microbiomes under warmer conditions, suggesting greater theoretical susceptibility to disturbance, as perturbations may propagate more readily across highly interconnected microbial networks.[47,50] These patterns align with pronounced compositional shifts in MP microbiomes, suggesting stronger environmental filtering, likely driven by temperature-dependent changes in MP surface properties. Increases in water temperatures and sunlight accelerate MP weathering and surface oxidation:[51,52] surface analyses have confirmed increased aging in specific polymer types and increased roughness across all MPs, causing polar functional group (e.g., hydroxyl, carbonyl) introduction and increasing surface hydrophilicity and chemical reactivity.[53] Under warmer conditions, therefore, MP microbiomes favor thermotolerant,[54] hydrophilic surface-associated taxa commonly found on weathered plastics (e.g., Firmicutes and Actinobacteria),[55,56] while cooler conditions favor hydrophobic surface-adapted taxa (e.g., Gammaproteobacteria).[57] Enhanced surface reactivity at higher temperatures promotes organic pollutant (e.g., polycyclic aromatic hydrocarbons,[58] antibiotics[59]) adsorption and plastic additive leaching.[60] These potential substrates or stressors[61] may favor microbes with functional traits involving complex carbon metabolism and resistance to environmental stresses. In contrast, NPs, which are primarily plant-derived, tend to present more nutrient-rich surfaces (e.g., cellulose and hemicellulose),[7,62,63] which may support more consistent microbial communities across the temperature gradient. These findings suggest that interactions between MP physicochemical properties and water temperature contribute to the unique composition of MP microbiomes and their divergence from those of NP microbiomes under warmer conditions.

PLS-PM analysis revealed that increasing water temperature increased the potential for both particle types to share microbial traits with RW, with MPs consistently showing a greater trait-sharing capacity. Warmer conditions enhanced the overlap of taxonomic indicators between MPs and RW, which frequently involved HGT to MP−RW-shared rMAGs and possibly altered native riverine microbiome compositions and functions. Several MP taxonomic indicators, including *Leuconostoc* spp. with known antibiotic resistance,[64] were uniquely shared with RW. Functional indicators related to stress tolerance, VFs, and ARGs were horizontally transferred from MP taxonomic indicators to MP−RW-shared rMAGs, suggesting the spread of MP-derived functional traits into RW ecosystems. These traits may be favored under warmer conditions as adaptive responses to temperature-induced changes in MP-specific surface properties,[65,66] promoting MP−RW trait sharing. In contrast, NP microbiomes shared fewer taxonomic and functional traits with RW, highlighting the unique role of MPs in shaping microbial and functional exchanges.

While this study highlights the temperature-dependent divergence between MP and NP microbiomes, several limitations should be acknowledged. First, we captured key spatial and seasonal trends in microbial dynamics at 15 representative sites in major subtropical urban rivers while controlling for site effects. However, the 1-year sampling duration hindered the evaluation of interannual variability and validation of the consistency of year-to-year observed seasonal trends across years. In addition, limited replication reduced the resolution for evaluating the within-site consistency. Future studies could broaden temporal and geographic coverage, including other climate zones, and incorporate within-site replication to more robustly assess seasonal dynamics and their generality. Second, water temperature emerged as the primary driver of microbiome divergence; however, other covarying environmental factors may also have contributed.[67] We also analyzed MPs and NPs as pooled groups without accounting for physicochemical properties (e.g., polymer type and particle size), possibly masking particle-specific microbial responses. Future studies should incorporate broader temperature ranges and control for particle characteristics to improve the generalizability. Third, although rMAGs provided important insights into microbial taxonomy, functional potential, and potential sharing, they are a small fraction of the total

https://doi.org/10.1021/acs.est.5c13903
Environ. Sci. Technol. 2026, 60, 14712−14725

metagenome and may not capture the full genomic and functional diversity. Deeper sequencing, short- and long-read integration, and optimized assembly strategies, combined with complementary classification and annotation approaches, are needed to enhance genome recovery and microbiome characterization resolution.[68] Lastly, microbial viability, activity, and ecological roles require experimental validation through complementary approaches, such as flow cytometric cell viability analysis,[69] antimicrobial susceptibility testing,[70] virulence assays,[71] and integrative omics (e.g., metatranscriptomics, metabolomics).[72] Additionally, quantitative methods (e.g., qPCR and flow cytometry) could be applied to enable absolute quantification of particle-associated microbial taxa and functional genes.[73] Experimental tracing of microbial dispersal through incubating fluorescently labeled cells with MPs, NPs, and in RW[74] would elucidate microbial sharing in aquatic environments.

Environmental Implications

Seasonal plastisphere dynamics must be understood to assess the long-term ecological impacts under changing environmental conditions.[75] Through year-round sampling of MPs and NPs in major urban rivers in densely populated Hong Kong, we identified water temperature as the primary driver of seasonal shifts in plastisphere composition. The observed temperature range (18−32 °C) reflects typical subtropical river conditions,[13] underscoring the broader relevance of these findings for warm climates. These data also are a useful reference for temperate or continental regions with broader water temperature fluctuations (e.g., ∼0−25 °C[76,77]), where microbial shifts may be even more pronounced, although patterns could vary with geographic and climatic contexts.[78] While we also observed temperature-driven changes in NP microbiomes, the unique physicochemical properties of MPs appeared to amplify the effects, increasing microbial divergence with warming and suggesting temperature-dependent ecological impacts of MPs in riverine ecosystems. Under warmer conditions in urban rivers, the plastisphere was enriched in taxa carrying pollutant degradation and putative virulence functions and metabolic capacities for diverse substrate utilization, which may influence aquatic nutrient cycling[79,80] and increase aquatic organisms' health risks through MP ingestion.[81,82] MPs consistently harbored higher putative PDE and ARG levels across the temperature gradient, suggesting that they act as stable reservoirs for specialized microbial functions[83] and facilitate the dissemination of these functions within aquatic ecosystems. These findings underscore the importance of incorporating thermal context, environmental variability, and long-term monitoring, particularly season-specific MP risk assessments in regions with fluctuating water temperatures, when evaluating plastispheres' ecological impacts. The data further suggest that prevailing studies, which often treat MPs as static isolated niches, may not fully capture their dynamic environmental interactions.[84−86]

We show that warming enhanced the spread of unique microbial traits, particularly putative virulence and antibiotic resistance, beyond MPs through microbial sharing and HGT, potentially reshaping the taxonomic and functional compositions of aquatic microbiomes. Warming also promoted microbial sharing between NPs and RW, suggesting that the more abundant NPs[26] may play an underrecognized ecological role. Nevertheless, MP-specific ecological risks may be exacerbated by continuing plastic pollution[87] and projected river warming (0.02−0.5 °C per decade).[88] Overall, our findings highlight temperature-dependent ecological risks unique to MPs and the plastisphere and provide key insights into the potential impacts of MP pollution on aquatic ecosystems under climate warming.

■ ASSOCIATED CONTENT

Supporting Information

The Supporting Information is available free of charge at https://pubs.acs.org/doi/10.1021/acs.est.5c13903.

Sample collection, particle characterization, and physicochemical analyses; metagenomic sequencing, bioinformatics, and taxonomic/functional analyses; rMAG cooccurrence network analysis; rMAG taxonomic/functional trait identification; microbial sharing and HGT event detection; PLS-PM analysis; data analysis and statistics; rMAG recovery and representativeness; environmental conditions; relative particle proportions by physical properties; O-PTIR signal intensities of MP plastic additives and aging; particle surface roughness; rMAG relative taxonomic/functional composition; db-RDA of environmental factor influences on microbiome composition; unique effects of individual environmental factors on taxonomic/functional diversity and functional redundancy; relationships between temperature intervals and taxonomic/functional similarity; effects of water temperature and particle type on network metrics and microbial ecological roles; temperature effects on network topology; top 5−10 most abundant genera among taxonomic indicators and functional indicator subcategories; seasonal variations of biofilm-related functions; seasonal associations between taxonomic and functional indicators; conceptual PLS-PM and structural equation model results (PDF)

Sampling sites and environmental data; PERMANOVA results of particle and microbiome compositions; rMAG quality metrics and taxonomy; associations between environmental factors and microbiome composition; Mantel test results between MP characteristics and microbiome compositions; network topological metrics; taxonomic/functional indicators; shared rMAGs; HGT functions from MP/NP indicators to other shared rMAGs; and PLS-PM path coefficients (XLSX)

■ AUTHOR INFORMATION

Corresponding Authors

James K. H. Fang − *Department of Food Science and Nutrition, The Hong Kong Polytechnic University, Hong Kong SAR, China; State Key Laboratory of Marine Environmental Health, City University of Hong Kong, Hong Kong SAR, China; Research Institute for Future Food, Research Centre for Resources Engineering towards Carbon Neutrality, and PolyU-BGI Joint Research Centre for Genomics and Synthetic Biology in Global Ocean Resources, The Hong Kong Polytechnic University, Hong Kong SAR, China*; Phone: (852) 3400-8703; Email: james.fang@polyu.edu.hk; Fax: (852) 2364-9909

Patrick K. H. Lee − *School of Energy and Environment and State Key Laboratory of Marine Environmental Health, City University of Hong Kong, Hong Kong SAR, China; Climate Impact and Environmental Resilience Research Center, City University of Hong Kong, Hong Kong SAR, China;*

orcid.org/0000-0003-0911-5317; Phone: (852) 3442-4625; Email: patrick.kh.lee@cityu.edu.hk; Fax: (852) 3442-0688

Authors

Yingyu Bao − *School of Energy and Environment and State Key Laboratory of Marine Environmental Health, City University of Hong Kong, Hong Kong SAR, China;* orcid.org/0000-0003-2233-6632

Yuen-Wa Ho − *Department of Food Science and Nutrition, The Hong Kong Polytechnic University, Hong Kong SAR, China; State Key Laboratory of Marine Environmental Health, City University of Hong Kong, Hong Kong SAR, China;* orcid.org/0000-0003-1523-112X

Zhiyong Shen − *School of Energy and Environment and State Key Laboratory of Marine Environmental Health, City University of Hong Kong, Hong Kong SAR, China*

Edmund Y. Lam − *Department of Electrical and Electronic Engineering, The University of Hong Kong, Hong Kong SAR, China;* orcid.org/0000-0001-6268-950X

Kenneth M. Y. Leung − *School of Energy and Environment and State Key Laboratory of Marine Environmental Health, City University of Hong Kong, Hong Kong SAR, China; Department of Chemistry, City University of Hong Kong, Hong Kong SAR, China;* orcid.org/0000-0002-2164-4281

Complete contact information is available at: https://pubs.acs.org/10.1021/acs.est.5c13903

Notes

The authors declare no competing financial interest.

■ ACKNOWLEDGMENTS

This research was supported by the Hong Kong Research Grants Council Research Impact Fund (R7003-21) and the Innovation and Technology Commission (ITC) of the Hong Kong SAR Government through regular research funding to the State Key Laboratory of Marine Environmental Health (SKLMEH-9448002). The views expressed herein are those of the authors and do not necessarily reflect the positions of the Hong Kong SAR Government or the ITC. We gratefully acknowledge Hewin T. H. Lo and Scott Y. S. Chui for their assistance with field sampling.

■ REFERENCES

(1) Gurnell, A.; Lee, M.; Souch, C. Urban rivers: hydrology, geomorphology, ecology and opportunities for change. *Geogr. Comp.* **2007**, *1* (5), 1118−1137.

(2) Moreno-Mateos, D.; Barbier, E. B.; Jones, P. C.; Jones, H. P.; Aronson, J.; López-López, J. A.; McCrackin, M. L.; Meli, P.; Montoya, D.; Rey Benayas, J. M. Anthropogenic ecosystem disturbance and the recovery debt. *Nat. Commun.* **2017**, *8* (1), No. 14163.

(3) Liang, Z.; Abdillah, A.; Fang, W.; Qiu, R.; Mai, B.; He, Z.; Juneau, P.; Gomes, M. P.; Priadi, C. R.; Wang, S. Unique microbiome in organic matter-polluted urban rivers. *Global Change Biol.* **2023**, *29* (2), 391−403.

(4) McCormick, A.; Hoellein, T. J.; Mason, S. A.; Schluep, J.; Kelly, J. J. Microplastic is an abundant and distinct microbial habitat in an urban river. *Environ. Sci. Technol.* **2014**, *48* (20), 11863−11871.

(5) Liu, X.; Wei, W.; Chen, Z.; Wu, L.; Duan, H.; Zheng, M.; Wang, D.; Ni, B.-J. The threats of micro- and nanoplastics to aquatic ecosystems and water health. *Nat. Water* **2025**, *3* (7), 764−781.

(6) Amaral-Zettler, L. A.; Zettler, E. R.; Mincer, T. J. Ecology of the plastisphere. *Nat. Rev. Microbiol.* **2020**, *18* (3), 139−151.

(7) Koelmans, A. A.; Redondo-Hasselerharm, P. E.; Nor, N. H. M.; de Ruijter, V. N.; Mintenig, S. M.; Kooi, M. Risk assessment of microplastic particles. *Nat. Rev. Mater.* **2022**, *7* (2), 138−152.

(8) Bao, Y.; Ho, Y.-W.; Shen, Z.; Lam, E. Y.; Fang, J. K. H.; Leung, K. M. Y.; Lee, P. K. H. Ecological Roles and Shared Microbes Differentiate the Plastisphere from Natural Particle-Associated Microbiomes in Urban Rivers. *Environ. Sci. Technol.* **2025**, *59* (32), 17298−17309.

(9) Wu, N. Tracing microplastic footprints through the plastisphere. *Nat. Rev. Earth Environ.* **2022**, *3* (8), 498.

(10) Anhwange, B.; Agbaji, E.; Gimba, E. Impact assessment of human activities and seasonal variation on River Benue, within Makurdi Metropolis. *Int. J. Sci. Technol. Res.* **2012**, *2* (5), 248−254.

(11) Adeyemo, O.; Adedokun, O.; Yusuf, R.; Abeleye, E. Seasonal changes in physico-chemical parameters and nutrient load of river sediments in Ibadan city, Nigeria. *Global Nest J.* **2008**, *10* (3), 326−336.

(12) Kodera, S. M.; Sharma, A.; Martino, C.; Dsouza, M.; Grippo, M.; Lutz, H. L.; Knight, R.; Gilbert, J. A.; Negri, C.; Allard, S. M. Microbiome response in an urban river system is dominated by seasonality over wastewater treatment upgrades. *Environ. Microbiome* **2023**, *18* (1), No. 10.

(13) Fang, W.; Fan, T.; Wang, S.; Yu, X.; Lu, A.; Wang, X.; Zhou, W.; Yuan, H.; Zhang, L. Seasonal changes driving shifts in microbial community assembly and species coexistence in an urban river. *Sci. Total Environ.* **2023**, *905*, No. 167027.

(14) Yu, Q.; Feng, T.; Yang, J.; Su, W.; Zhou, R.; Wang, Y.; Zhang, H.; Li, H. Seasonal distribution of antibiotic resistance genes in the Yellow River water and tap water, and their potential transmission from water to human. *Environ. Pollut.* **2022**, *292*, No. 118304.

(15) Yuan, B.; Guo, M.; Wu, W.; Zhou, X.; Li, M.; Xie, S. Spatial and seasonal patterns of sediment bacterial communities in large river cascade reservoirs: drivers, assembly processes, and co-occurrence relationship. *Microb. Ecol.* **2023**, *85* (2), 586−603.

(16) Oberbeckmann, S.; Loeder, M. G.; Gerdts, G.; Osborn, A. M. Spatial and seasonal variation in diversity and structure of microbial biofilms on marine plastics in Northern European waters. *FEMS Microbiol. Ecol.* **2014**, *90* (2), 478−492.

(17) Yang, Y.; Chen, C.; Yao, K.; Grossart, H.-P. Seasonal dynamics of free-living (FL) and particle-attached (PA) bacterial communities in a plateau reservoir. *Front. Microbiol.* **2024**, *15*, No. 1428701.

(18) Villalba, L. A.; Karnatak, R.; Grossart, H. P.; Wollrab, S. Flexible habitat choice of pelagic bacteria increases system stability and energy flow through the microbial loop. *Limnol. Oceanogr.* **2022**, *67* (6), 1402−1415.

(19) Su, Y.; Hu, X.; Tang, H.; Lu, K.; Li, H.; Liu, S.; Xing, B.; Ji, R. Steam disinfection releases micro (nano) plastics from silicone-rubber baby teats as examined by optical photothermal infrared microspectroscopy. *Nat. Nanotechnol.* **2022**, *17* (1), 76−85.

(20) Zhou, T.; Wu, J.; Liu, Y.; Xu, A. Seawater accelerated the aging of polystyrene and enhanced its toxic effects on Caenorhabditis elegans. *Int. J. Mol. Sci.* **2023**, *24* (24), No. 17219.

(21) Malik, A. A.; Martiny, J. B. H.; Brodie, E. L.; Martiny, A. C.; Treseder, K. K.; Allison, S. D. Defining trait-based microbial strategies with consequences for soil carbon cycling under climate change. *ISME J.* **2020**, *14* (1), 1−9.

(22) Raveh-Sadka, T.; Firek, B.; Sharon, I.; Baker, R.; Brown, C. T.; Thomas, B. C.; Morowitz, M. J.; Banfield, J. F. Evidence for persistent and shared bacterial strains against a background of largely unique gut colonization in hospitalized premature infants. *ISME J.* **2016**, *10* (12), 2817−2830.

(23) Raveh-Sadka, T.; Thomas, B. C.; Singh, A.; Firek, B.; Brooks, B.; Castelle, C. J.; Sharon, I.; Baker, R.; Good, M.; Morowitz, M. J.; Banfield, J. F. Gut bacteria are rarely shared by co-hospitalized premature infants, regardless of necrotizing enterocolitis development. *eLife* **2015**, *4*, No. e05477.

(24) Team, R. C. R: A language and environment for statistical computing. In *R Foundation for Statistical Computing* Vienna, 2022.

(25) Yu, J.; Lee, J. Y. Y.; Tang, S. N.; Lee, P. K. H. Niche differentiation in microbial communities with stable genomic traits over time in engineered systems. *ISME J.* **2024**, *18* (1), No. wrae042.
(26) Hochella, M. F.; Mogk, D. W.; Ranville, J.; Allen, I. C.; Luther, G. W.; Marr, L. C.; McGrail, B. P.; Murayama, M.; Qafoku, N. P.; Rosso, K. M.; et al. Natural, incidental, and engineered nanomaterials and their impacts on the Earth system. *Science* **2019**, *363* (6434), No. eaau8299.
(27) McLellan, S. L.; Boehm, A. B.; Shanks, O. C. Marine and freshwater fecal indicators and source identification. In *Infectious Diseases: Selected Entries from the Encyclopedia of Sustainability Science and Technology*; Springer, 2012; pp 199−235.
(28) Behera, S.; Das, S. Potential and prospects of Actinobacteria in the bioremediation of environmental pollutants: Cellular mechanisms and genetic regulations. *Microbiol. Res.* **2023**, *273*, No. 127399.
(29) Shen, X.-H.; Zhou, N.-Y.; Liu, S.-J. Degradation and assimilation of aromatic compounds by Corynebacterium glutamicum: another potential for applications for this bacterium? *Appl. Microbiol. Biotechnol.* **2012**, *95*, 77−89.
(30) Chhetri, G.; Kim, H.-J.; Jeon, J.-M.; Yoon, J.-J. Isolation of Massilia species capable of degrading Poly(3-hydroxybutyrate) isolated from eggplant (Solanum melongena L.) field. *Chemosphere* **2024**, *368*, No. 143776.
(31) Sharma, S.; Pathak, H. Pseudomonas in biodegradation. *Int. J. Pure Appl. Biosci.* **2014**, *2* (2), 213−222.
(32) Lyu, L.; Fang, K.; Huang, X.; Tian, X.; Zhang, S. Polyethylene is degraded by the deep-sea Acinetobacter venetianus bacterium. *Environ. Chem. Lett.* **2024**, *22* (4), 1591−1597.
(33) Tripathy, B.; Sahoo, P. P.; Sundaray, H.; Das, A. P. In-vitro biodegradation of discarded marine microplastics across the eastern coast of the Bay of Bengal, India using Exiguobacterium sp. *Environ. Chem. Ecotoxicol.* **2024**, *6*, 236−247.
(34) Salam, L. B.; Obayori, O. S.; Olatoye, N. O. Biodegradation of anthracene by a novel actinomycete, Microbacterium sp. isolated from tropical hydrocarbon-contaminated soil. *World J. Microbiol. Biotechnol.* **2014**, *30*, 335−341.
(35) Asaf, S.; Numan, M.; Khan, A. L.; Al-Harrasi, A. Sphingomonas: from diversity and genomics to functional role in environmental remediation and plant growth. *Crit. Rev. Biotechnol.* **2020**, *40* (2), 138−152.
(36) Pipes, W. O.; Jones, P. Decomposition of organic wastes by Sphaerotilus. *Biotechnol. Bioeng.* **1963**, *5* (4), 287−307.
(37) Fan, Y.; Zheng, J.; Deng, L.; Rao, W.; Zhang, Q.; Liu, T.; Qian, X. Spatiotemporal dynamics of microplastics in an urban river network area. *Water Res.* **2022**, *212*, No. 118116.
(38) Jousset, A.; Eisenhauer, N.; Merker, M.; Mouquet, N.; Scheu, S. High functional diversity stimulates diversification in experimental microbial communities. *Sci. Adv.* **2016**, *2* (6), No. e1600124.
(39) Downing, J. A. Productivity of Freshwater Ecosystems and Climate Change. In *Global Environmental Change*; Freedman, B., Ed.; Springer Netherlands: Dordrecht, 2014; pp 221−229.
(40) Claire Horner-Devine, M.; Leibold, M. A.; Smith, V. H.; Bohannan, B. J. Bacterial diversity patterns along a gradient of primary productivity. *Ecol. Lett.* **2003**, *6* (7), 613−622.
(41) Smith, T. P.; Thomas, T. J.; García-Carreras, B.; Sal, S.; Yvon-Durocher, G.; Bell, T.; Pawar, S. Community-level respiration of prokaryotic microbes may rise with global warming. *Nat. Commun.* **2019**, *10* (1), No. 5124.
(42) Liu, Y.; Guo, W.; Wei, C.; Huang, H.; Nan, F.; Liu, X.; Liu, Q.; Lv, J.; Feng, J.; Xie, S. Rainfall-induced changes in aquatic microbial communities and stability of dissolved organic matter: Insight from a Fen river analysis. *Environ. Res.* **2024**, *246*, No. 118107.
(43) Wéry, N.; Monteil, C.; Pourcher, A.-M.; Godon, J.-J. Human-specific fecal bacteria in wastewater treatment plant effluents. *Water Res.* **2010**, *44* (6), 1873−1883.
(44) Tian, L.; Wang, X.-W.; Wu, A.-K.; Fan, Y.; Friedman, J.; Dahlin, A.; Waldor, M. K.; Weinstock, G. M.; Weiss, S. T.; Liu, Y.-Y. Deciphering functional redundancy in the human microbiome. *Nat. Commun.* **2020**, *11* (1), No. 6217.
(45) Louca, S.; Polz, M. F.; Mazel, F.; Albright, M. B.; Huber, J. A.; O'Connor, M. I.; Ackermann, M.; Hahn, A. S.; Srivastava, D. S.; Crowe, S. A.; et al. Function and functional redundancy in microbial systems. *Nat. Ecol. Evol.* **2018**, *2* (6), 936−943.
(46) Herren, C. M.; McMahon, K. D. Cohesion: a method for quantifying the connectivity of microbial communities. *ISME J.* **2017**, *11* (11), 2426−2438.
(47) Hernandez, D. J.; David, A. S.; Menges, E. S.; Searcy, C. A.; Afkhami, M. E. Environmental stress destabilizes microbial networks. *ISME J.* **2021**, *15* (6), 1722−1734.
(48) Ebrahimi, A.; Goyal, A.; Cordero, O. X. Particle foraging strategies promote microbial diversity in marine environments. *eLife* **2022**, *11*, No. e73948.
(49) Albright, M. B. N.; Sevanto, S.; Gallegos-Graves La, V.; Dunbar, J. Biotic Interactions Are More Important than Propagule Pressure in Microbial Community Invasions. *mBio* **2020**, *11* (5), No. e02089−20.
(50) Stouffer, D. B.; Bascompte, J. Compartmentalization increases food-web persistence. *Proc. Natl. Acad. Sci. U.S.A.* **2011**, *108* (9), 3648−3652.
(51) Rajakumar, K.; Sarasvathy, V.; Thamarai Chelvan, A.; Chitra, R.; Vijayakumar, C. Natural weathering studies of polypropylene. *J. Polym. Environ.* **2009**, *17*, 191−202.
(52) Masry, M.; Rossignol, S.; Gardette, J.-L.; Therias, S.; Bussière, P.-O.; Wong-Wah-Chung, P. Characteristics, fate, and impact of marine plastic debris exposed to sunlight: A review. *Mar. Pollut. Bull.* **2021**, *171*, No. 112701.
(53) Duan, J.; Bolan, N.; Li, Y.; Ding, S.; Atugoda, T.; Vithanage, M.; Sarkar, B.; Tsang, D. C.; Kirkham, M. Weathering of microplastics and interaction with other coexisting constituents in terrestrial and aquatic environments. *Water Res.* **2021**, *196*, No. 117011.
(54) Flores-Piña, A.; Valencia-Cantero, E.; Santoyo, G. Underground fires shape the structure of microbial communities and select for thermophilic bacteria through a temperature gradient. *Microbiol. Res.* **2025**, *292*, No. 127996.
(55) Tao, X.; Ouyang, H.; Zhou, A.; Wang, D.; Matlock, H.; Morgan, J. S.; Ren, A. T.; Mu, D.; Pan, C.; Zhu, X.; et al. Polyethylene degradation by a Rhodococcous strain isolated from naturally weathered plastic waste enrichment. *Environ. Sci. Technol.* **2023**, *57* (37), 13901−13911.
(56) Bao, R.; Cheng, Z.; Hou, Y.; Xie, C.; Pu, J.; Peng, L.; Gao, L.; Chen, W.; Su, Y. Secondary microplastics formation and colonized microorganisms on the surface of conventional and degradable plastic granules during long-term UV aging in various environmental media. *J. Hazard. Mater.* **2022**, *439*, No. 129686.
(57) Harrison, J. P.; Schratzberger, M.; Sapp, M.; Osborn, A. M. Rapid bacterial colonization of low-density polyethylene microplastics in coastal sediment microcosms. *BMC Microbiol.* **2014**, *14* (1), 1−15.
(58) Wang, Z.; Chen, M.; Zhang, L.; Wang, K.; Yu, X.; Zheng, Z.; Zheng, R. Sorption behaviors of phenanthrene on the microplastics identified in a mariculture farm in Xiangshan Bay, southeastern China. *Sci. Total Environ.* **2018**, *628-629*, 1617−1626.
(59) Liu, P.; Qian, L.; Wang, H.; Zhan, X.; Lu, K.; Gu, C.; Gao, S. New Insights into the Aging Behavior of Microplastics Accelerated by Advanced Oxidation Processes. *Environ. Sci. Technol.* **2019**, *53* (7), 3579−3588.
(60) Dimassi, S. N.; Hahladakis, J. N.; Yahia, M. N. D.; Ahmad, M. I.; Sayadi, S.; Al-Ghouti, M. A. Effect of temperature and sunlight on the leachability potential of BPA and phthalates from plastic litter under marine conditions. *Sci. Total Environ.* **2023**, *894*, No. 164954.
(61) Yu, Y.; Kumar, M.; Bolan, S.; Padhye, L. P.; Bolan, N.; Li, S.; Wang, L.; Hou, D.; Li, Y. Various additive release from microplastics and their toxicity in aquatic environments. *Environ. Pollut.* **2024**, *343*, No. 123219.
(62) Santos-Júnior, C. D.; Sarmento, H.; de Miranda, F. P.; Henrique-Silva, F.; Logares, R. Uncovering the genomic potential of the Amazon River microbiome to degrade rainforest organic matter. *Microbiome* **2020**, *8* (1), No. 151.

(63) Di Blasi, C.; Signorelli, G.; Di Russo, C.; Rea, G. Product distribution from pyrolysis of wood and agricultural residues. *Ind. Eng. Chem. Res.* **1999**, *38* (6), 2216−2224.
(64) Ogier, J. C.; Casalta, E.; Farrokh, C.; Saïhi, A. Safety assessment of dairy microorganisms: the Leuconostoc genus. *Int. J. Food Microbiol.* **2008**, *126* (3), 286−290.
(65) Zhu, S.; Hong, J.; Wang, T. Horizontal gene transfer is predicted to overcome the diversity limit of competing microbial species. *Nat. Commun.* **2024**, *15* (1), No. 800.
(66) Zhao, W.; Zhang, B.; Zheng, S.; Yan, W.; Yu, X.; Ye, C. High temperatures promote antibiotic resistance genes conjugative transfer under residual chlorine: Mechanisms and risks. *J. Hazard. Mater.* **2025**, *483*, No. 136675.
(67) Kirschbaum, M. U. Seasonal variations in the availability of labile substrate confound the temperature dependence of organic matter decomposition. *Soil Biol. Biochem.* **2013**, *57*, 568−576.
(68) Amarasinghe, S. L.; Su, S.; Dong, X.; Zappia, L.; Ritchie, M. E.; Gouil, Q. Opportunities and challenges in long-read sequencing data analysis. *Genome Biol.* **2020**, *21* (1), No. 30.
(69) Wilkinson, M. G. Flow cytometry as a potential method of measuring bacterial viability in probiotic products: A review. *Trends Food Sci. Technol.* **2018**, *78*, 1−10.
(70) Abdolahpur Monikh, F.; Baun, A.; Hartmann, N. B.; Kortet, R.; Akkanen, J.; Lee, J.-S.; Shi, H.; Lahive, E.; Uurasjärvi, E.; Tufenkji, N.; et al. Exposure protocol for ecotoxicity testing of microplastics and nanoplastics. *Nat. Protoc.* **2023**, *18* (11), 3534−3564.
(71) Chebotar, I.; Azizov, I.; Edelstein, M.; Kozlov, R. Detection of virulence factors in opportunistic bacteria: advances, challenges, and practical implementation. *Front. Microbiol.* **2025**, *16*, No. 1638925.
(72) Aguiar-Pulido, V.; Huang, W.; Suarez-Ulloa, V.; Cickovski, T.; Mathee, K.; Narasimhan, G. Metagenomics, Metatranscriptomics, and Metabolomics Approaches for Microbiome Analysis. *Evol. Bioinform. Online* **2016**, *12s1*, 5−16.
(73) Barlow, J. T.; Bogatyrev, S. R.; Ismagilov, R. F. A quantitative sequencing framework for absolute abundance measurements of mucosal and lumenal microbial communities. *Nat. Commun.* **2020**, *11* (1), No. 2590.
(74) Jorrin, B.; Haskett, T. L.; Knights, H. E.; Martyn, A.; Underwood, T. J.; Dolliver, J.; Ledermann, R.; Poole, P. S. Stable, fluorescent markers for tracking synthetic communities and assembly dynamics. *Microbiome* **2024**, *12* (1), No. 81.
(75) Miao, L.; Li, W.; Adyel, T. M.; Yao, Y.; Deng, Y.; Wu, J.; Zhou, Y.; Yu, Y.; Hou, J. Spatio-temporal succession of microbial communities in plastisphere and their potentials for plastic degradation in freshwater ecosystems. *Water Res.* **2023**, *229*, No. 119406.
(76) Goldenberg-Vilar, A.; Morán-Luis, M.; Vieites, D. R.; Álvarez-Martínez, J. M.; Silió, A.; Mony, C.; Varandas, S.; Monteiro, S. M.; Burgess, D.; Cabecinha, E.; Barquín, J. Biogeographical Distribution of River Microbial Communities in Atlantic Catchments. *Environ. Microbiol. Rep.* **2025**, *17* (1), No. e70065.
(77) Syvitski, J.; Cohen, S.; Miara, A.; Best, J. River temperature and the thermal-dynamic transport of sediment. *Global Planet. Change* **2019**, *178*, 168−183.
(78) Marsay, K. S.; Ambrosino, A. C.; Koucherov, Y.; Davidov, K.; Figueiredo, N.; Yakovenko, I.; Itzahri, S.; Martins, M.; Sobral, P.; Oren, M. The geographical and seasonal effects on the composition of marine microplastic and its microbial communities: The case study of Israel and Portugal. *Front. Microbiol.* **2023**, *14*, No. 1089926.
(79) Huang, W.; Xia, X. Element cycling with micro nano) plastics. *Science* **2024**, *385* (6712), 933−935.
(80) Mincer, T. J.; Zettler, E. R.; Amaral-Zettler, L. A. Biofilms on Plastic Debris and Their Influence on Marine Nutrient Cycling, Productivity, and Hazardous Chemical Mobility. In *Hazardous Chemicals Associated with Plastics in the Marine Environment*; Takada, H.; Karapanagioti, H. K., Eds.; Springer International Publishing: Cham, 2019; pp 221−233.
(81) Bowley, J.; Baker-Austin, C.; Porter, A.; Hartnell, R.; Lewis, C. Oceanic hitchhikers−assessing pathogen risks from marine microplastic. *Trends Microbiol.* **2021**, *29* (2), 107−116.
(82) Yan, Z.; Hao, Z.; Zhang, Z.; Liu, R.; Zhao, K.; Zhang, Y. A Noninvasive Quantitative Method for Evaluating Intestinal Exposure to Microplastics Based on the Excretion and Metabolism Patterns of Microplastics and Their Additives. *Environ. Sci. Technol.* **2024**, *58* (18), 7791−7801.
(83) Wright, R. J.; Langille, M. G. I.; Walker, T. R. Food or just a free ride? A meta-analysis reveals the global diversity of the Plastisphere. *ISME J.* **2021**, *15* (3), 789−806.
(84) Li, C.; Gillings, M. R.; Zhang, C.; Chen, Q.; Zhu, D.; Wang, J.; Zhao, K.; Xu, Q.; Leung, P. H.; Li, X.; Liu, J.; Jin, L. Ecology and risks of the global plastisphere as a newly expanding microbial habitat. *Innovation* **2024**, *5* (1), No. 100543.
(85) Delacuvellerie, A.; Géron, A.; Gobert, S.; Wattiez, R. New insights into the functioning and structure of the PE and PP plastispheres from the Mediterranean Sea. *Environ. Pollut.* **2022**, *295*, No. 118678.
(86) Zhang, J.; Shao, Y.; Li, Z.; Han, G.; Jing, X.; Wang, N.; Xu, J.; Chen, G. Characteristics analysis of plastisphere biofilm and effect of aging products on nitrogen metabolizing flora in microcosm wetlands experiment. *J. Hazard. Mater.* **2023**, *452*, No. 131336.
(87) Windsor, F. M.; Durance, I.; Horton, A. A.; Thompson, R. C.; Tyler, C. R.; Ormerod, S. J. A catchment-scale perspective of plastic pollution. *Global Change Biol.* **2019**, *25* (4), 1207−1221.
(88) Liu, S.; Xie, Z.; Liu, B.; Wang, Y.; Gao, J.; Zeng, Y.; Xie, J.; Xie, Z.; Jia, B.; Qin, P.; Li, R.; Wang, L.; Chen, S. Global river water warming due to climate change and anthropogenic heat emission. *Global Planet. Change* **2020**, *193*, No. 103289.

https://doi.org/10.1021/acs.est.5c13903
Environ. Sci. Technol. 2026, 60, 14712−14725